From hyperspectral imaging to dedicated sensors

Eric J. Bakker, Piet B.W. Schwering, and Sebastiaan P. van den Broek

TNO Physics and Electronics Laboratory, P.O. Box 96864, 2509 JG The Hague, The Netherlands

ABSTRACT

Hyper spectral imaging is a technique that obtains a two-dimensional image of a scene, while for each pixel a spectrum is recorded. Hyper spectral imaging systems can be very powerful at extracting information by using the spectral information in addition to the more conventional information extraction algorithms based on the spatial information within an image. However it is very unlikely that a hyper spectral imager will be used as a sensor for day to day operations. Hyper spectral imagers have the disadvantage of being rather complex and generating huge amounts of data. In this paper we discuss the approach that hyper spectral imagers are most powerful as research instruments and that they can be used to develop dedicated sensors for a particular application. Such a dedicated sensor could be optimized by selecting the most appropriate wavelength bands and making these bands as broad, or as narrow, as needed in order to detect, classify, or identify targets. The number of bands needed for such a dedicated sensor may depend on the accepted false alarm rate of such a system. In this paper we present some example spectra of materials and atmospheric transmission and discuss how a dedicated sensor can be designed for a specific application.

Keywords: hyper spectral imagery, infrared spectra, atmospheric transmission, dedicated sensors

1. INTRODUCTION

Photons emitted or reflected by an object and recorded by a sensor contain a wealth of information. Three dimensions of information can be distinguished. The recorded radiation contains information on the shape and size of a objects (the spatial domain), the reflection and emission efficiency of the surface of the objects (spectral domain, which includes polarization and bi-directional reflectance distribution), and information on time variations, e.g., speed and temperature variability (the temporal domain). Each sensor is designed for a specific task and has an optimum position in the spatial-spectral-temporal information space. For example, a sensor optimized for spatial resolution has a small instantaneous field of view and a large number of pixels. A sensor optimized for spectral resolution records a single pixel spectrum of an object with a spectral resolution as high as possible. A sensor designed for temporal resolution is a very sensitive single point detector element such that short exposures provide sufficient signal. Furthermore, sensor limitations are based on operational constraints of field of view, data rate, spectral band, size, and cost. Spectral discrimination techniques have been proposed for several decades [1], and they could now become available with the launch of hyper spectral imagers. Spectral imagery is a technique that aims at extracting as much spectral information from a scene as possible. A spectral imager is designed to be a compromise between spatial, spectral, and temporal resolution (Figure 1). A spectral imagery dataset contains therefore four dimensional data: two spatial dimensions (x, and y), the spectral dimension (λ for each x, y), and the temporal domain (t for each x, y, and λ).

The adjective "hyper" refers to the spectral domain. While multi spectral imaging systems have a small number of (non-) adjacent spectral bins (typically 8 bands) with low spectral resolution ($\Delta\lambda > 100$ nm at 5 μm), hyper spectral imaging systems have a larger number of adjacent spectral bins (typically 100 to 500 bands) with moderate spectral resolution ($\Delta\lambda \approx$ 10 - 100 nm at 5 μm). Ultra-spectral imagers have a larger number of adjacent spectral bins (larger than about 500 bands), and high spectral resolution ($\Delta\lambda < 10$ nm at 5 μm). An officially adopted definition of these terms is not available and different authors use different definitions. In this paper we are concerned with hyper spectral imagers.

The obvious advantage of a hyper spectral imager with respect to a traditional camera system is that information from the spectral domain is recorded. This facilitates target detection and classification. The disadvantage of a hyper spectral imager is that the system is complex, expensive, and that the recording speed of the system is inversely proportional to the number of spectral bins recorded: a hyper spectral imager with 250 channels takes 250 images, while a traditional camera records only a single image of the same dimensions. This causes a increase in recording speed (exposure time to record one data cube) by a factor 250, or a decrease in signal-to-noise ratio of a factor $\sqrt{250}$. Because of this, it is foreseen that hyper spectral imagers will mostly be used for research purposes in order to develop dedicated multi spectral sensors [2]. TNO has

In *Targets and Backgrounds VI: Characterization, Visualization, and the Detection Process*, Wendell R. Watkins, Dieter Clement, William R. Reynolds, Editors, Proceedings of SPIE Vol. 4029 (2000) • 0277-786X/00/$15.00

long (since the 1980's) been a player in the field of spectroscopy and has all the tools available to develop dedicated multi spectral sensor systems [3].

In this paper we elaborate on potential applications of a hyper spectral imager in order to develop simple and low-cost dedicated sensors that can identify a target by using a small number of spectral bands. A critical issue is the preferred wavelength range for the hyper spectral imager and the dedicated sensor. This first of all depends on the kind of operational application one has in mind. In the following section we elaborate on applications, followed by a short study on spectral characteristics of man-made objects and their natural environment, followed by a study on atmospheric transmission in the infrared. TNO offers an end-to-end approach to electro-optical questions. As hyper spectral imaging and the developed dedicated sensors offer improved capabilities to detect, classify, and identify targets, this also poses new challenges for camouflage and countermeasures. A discussion is presented which aims at providing a vision on hyper spectral imaging and dedicated sensors for the near and far future.

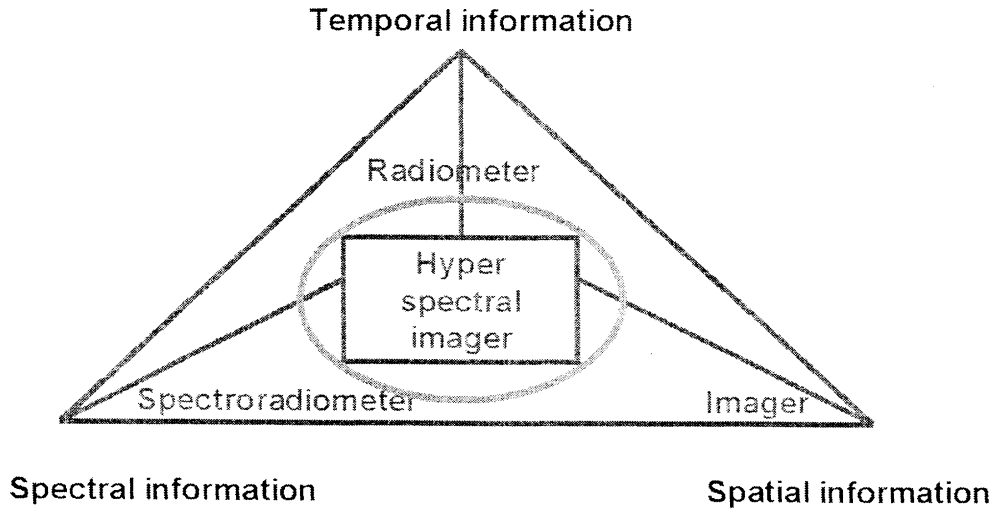

Figure 1: **schematical presentation of spatial-spectral-temporal information space for radiation.**

2. APPLICATIONS

Currently commercially available hyper spectral imagers are scanning. Some of the imagers scan the spectrum by means of a filter, others take the spectrum instantaneous, but scan the image with a scanning mirror, while still others scan the Fourier domain. None of the currently available commercial hyper spectral imagers are non-scanning (although this is technologically feasibly and quite challenging). This limitation leads to long exposure times before a scene has been recorded at sufficient spatial and spectral resolution at sufficient signal-to-noise ratio. Temporal resolution is sacrificed leading to exposures from seconds to several minutes. Hence the best applications are those for which objects in the scene are stationary during the exposure time.

This therefore prefers land-based and sea-surface based scenes above those with air-borne targets. From a scientific point of view the land-based application is of most interest as the background is rather diverse, but show little temporal variability. An example is an object (e.g., car) in a vegetation landscape. The maritime scenario also has interesting potential, based on background differences and the sun glint influence on false alarms. Examples of CATSI spectral measurements [4] showing the variation of the sky and sea background in the Mediterranean near Crete are given with elevation at nearly grazing angles. In general the high variability of background spectral data in these scenarios could be beneficial in separating targets from background clutter.

3. SYSTEM CONSIDERATIONS

The use of a hyper spectral imager is basically aimed to optimize sensor systems to use sub-bands of the mid-wave or long-wave infrared atmospheric windows, among which the Infrared Search and Track (IRST) systems and Forward Looking InfraRed (FLIR) imagers. This optimization may be done in the field of sensor heads and data processing. Obviously, data reduction (by using the minimum number of spectral bands) in an early stage will be advantageous due to the enormous amount of data created by a hyper spectral imager. Hence, sub-band selection and optical processing are methods for application in final system design.

The application of dedicated sensors for military applications can be divided in two categories. Those that are used for target detection (the target is at a larger distance and is seen as a point source), and those that are used to classify or identify an already detected target (the target is at short distance and spatial details can be identified).

Target detection: to enhance the detection process, the main use of hyper spectral imaging will come from optimizing the effective sensor bandwidth for expected target-to-background and target-to-noise contrast. Under these low signal-to-background ratio scenarios the aim is to maintain or optimize sufficient contrast in the chosen sub-band. Hence long-term research into these contrast aspects is of vital importance to optimize sensors of the future. An example of such a system is a missile warning system that searches the skies for incoming missiles using a filter centered on the red and blue spike of CO_2 emission from the plume of the missile (see Figure 5 for a plume spectrum).

Target classification: for the classification and identification process, detection has already taken place and the stripping of all photons in small spectral bands may become useful in the classification process. Due to the stronger signals the closer range makes classification in particular spectral features evident. Furthermore the spectral characteristics may optimize the already available passive range methods by making use of hyper spectral atmospheric extinction effects. An example of such a system is a sensor that makes a distinction between the paint applied to a target for a friend or foe identification.

Backgrounds: in target detection and classification systems the major feature is the target-to-clutter and target-to-noise contrast ratio. Depending on sensor noise or background clutter dominance, the highest contrast ratio should be obtained for best data analysis and target processing. Effective target classification algorithms should therefore be based on spectral knowledge of targets, false targets, camouflage information, atmosphere, and backgrounds. In particular the spectral knowledge on backgrounds can be widely varying and may become dominant in many cases. First of all we are dealing with many different types of backgrounds spectra such as sand, grass, water with reflected sky and sun glints, etc. In all scenarios spatial variations in the background occur. In particular situations, such as those with moving targets or moving background, structure temporal fluctuations of the spectra occur. Obviously, the spectral content inside a four-dimensional (2 spatial, 1 temporal, and 1 spectral axis) data cube needs to be optimized for classification. Hence, in cases of background limited performance, background data plays a dominant role.

4. SPECTRAL SIGNATURES

Hyper spectral imagers have the disadvantage of generating large amounts of data. Because of that we believe a detailed study on laboratory and field spectra of a single point target is beneficial to obtain in depth knowledge on spectral features. To support hyper spectral imaging activities TNO-FEL is developing a spectral database referred to as SPEKY that contains spectra obtained under controlled circumstances.

Laboratory spectra were obtained with a Shimadzu UV 3100 in combination with multi-purpose compartment (for reflection measurements) MPC 3100 for measurements in the visible and near-infrared (190 nm to 2600 nm). Infrared spectra were obtained with a Shimadzu FTIR 8101M in combination with a second sample unit with a liquid nitrogen cooled HgCdTe detector SSU-8000 (400 cm^{-1} to 4600 cm^{-1}). These two spectrometers combined allow recording spectra from 190 nm to 25 μm. Spectra are recorded at a spectral resolution of 12 nm in the ultraviolet and visible, and 4 cm^{-1} in the infrared. Each sample is measured multiple times at different occasions.

Additionally, field spectra were recorded with a BOMEM MR254 (1700 cm^{-1} to 7000 cm^{-1}) at a spectral resolution most appropriate for the target (depending on expected signal, but typically 4 cm^{-1}). A selection of spectra (Figures 2, 3, 4, and 5) is presented in this paper. These spectra are part of a spectral database (referred to as SPEKY), which is under development at TNO-FEL. This database is aimed at collecting spectra in support of hyper spectral imaging activities.

In the remainder of this section an empirical (phenomenological) description of the spectra is presented. The laboratory spectra are presented as reflection spectra, the field spectra as emission spectra.

For an ideal reflector the reflection coefficient equals R = 100 %, and the reflection spectra will be discussed in term of not being a perfect reflector. An ideal blackbody would have a reflection coefficient of 0 % (emissivity of E = 100 %). Assuming that the samples used do not transmit radiation (T = 0 %), the emissivity is equal to E = 100 % minus the reflectivity R. Using a formulae this can be described as E (%) + T (%) + R (%) = 100 %. For T = 0 %, then E (%) = 100 % - R(%). A minimum in the reflection spectra will be referred to as an absorption feature.

Laboratory spectra: laboratory spectra are obtained from a piece of blue paper and a piece of plastic (with two different paints applied to it). From a first look at the laboratory spectra presented in Figures 2 and 3 we note that the absolute value of the infrared reflection coefficient for different spectra obtained for a sample is not constant. Although the positions of features remain the same, the absolute scale varies. The explanation for the absolute differences in reflection coefficient in the infrared is a result of intrinsic small-scale variations of the sample and alignment of the system. In the infrared spectrometer the infrared beam is focussed on the target. The reflected radiation is directed towards the detector. As not all samples have the same thickness, the sample cannot always be placed at this focus point. If the sample is not exactly at this focus point the infrared beam is slightly misaligned. As a result, the incident beam on the detector will not be in focus and the resulting spot size will be larger than it should be. Hence the absolute intensity decreases. In the future we will solve this problem by using a custom-made sample holder which will eliminate this problem. In conclusion, the spectral features presented can be trusted, the absolute scale has an uncertainty of approximately 20 %.

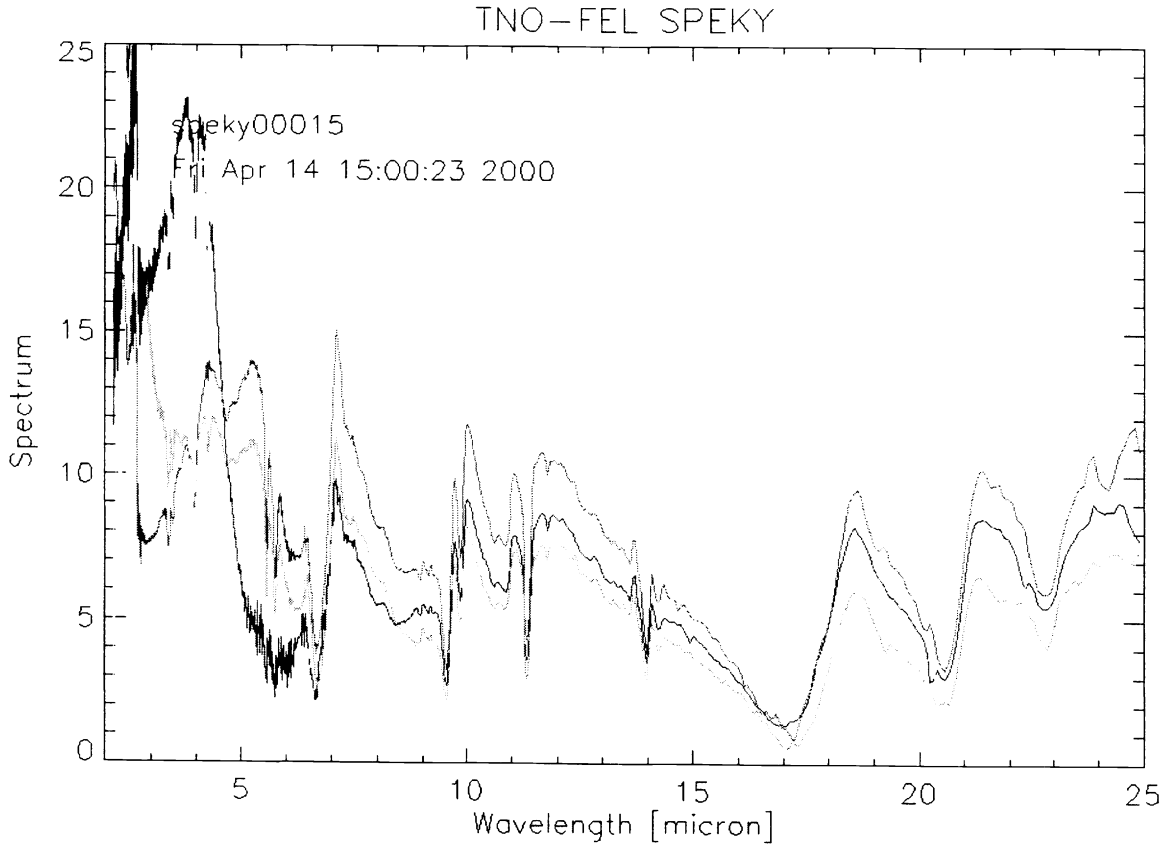

Figure 2: **spectra of blue paper (reflection coefficient in % versus wavelength from 2 μm to 25 μm).**

In Figure 2, seven (four infrared) spectra of one and the same piece of blue paper (the blue color of the TNO logo) are presented. As already noted the absolute scale of the reflection spectrum shows significant variations that are attributed to

small-scale efficiency variations of the sample and mis-alignment of the system. The spectral features are due to molecules present within the paper and are possibly unique for this paint or paper. Based on Figure 2 we note:

1. There are a number of distinct spectral features present
   1.1. narrow absorption features are present at: 3.4, 4.0, 5.6, 5.8, 8.9, 9.2, 9.5, 9.9, 11.3, 11.8, 14.0, and 14.3 μm, with a typical full-width-half-maximum of 0.05 μm;
   1.2. broad absorption features are present at 4.8, 6.2, 6.7, 10.8, 17.1, 20.5, and 22.8 μm with a typical full-width-half-maximum of 0.5 μm;
2. These features occur in each of the presented spectra although shapes do vary somewhat. At this stage we do have some suggestions for assignments: 3.4 μm C-H stretch; the 22.8 μm, 20.5 μm, and 17.1 μm features seem to form a sequence suggesting one molecule responsible. Also the asymmetry of these lines suggest one origin;
3. The spectrum between 2 μm and 7 μm changes significantly in shape. Some spectra have a low reflection coefficient near 4 μm (R ≅ 10 %) and the spectrum rises from 3 μm to 5 μm. Other spectra have a peak near 4 μm (R ≅ 20 %) and the spectrum falls from 4 μm to 6 μm. Spectra belonging to these two groups have been taken at different occasions. Hence the chemical composition or the condition of the paper must have changed between these two occasions. This change in chemical composition or conditions could be related to the temperature, humidity, or some kind of out gassing of the paper or degradation of the paint. From a scientific point of view this is a rather intriguing question as changes in the shape of the reflection spectrum might be used as a measure of a physical process or state of the paper.

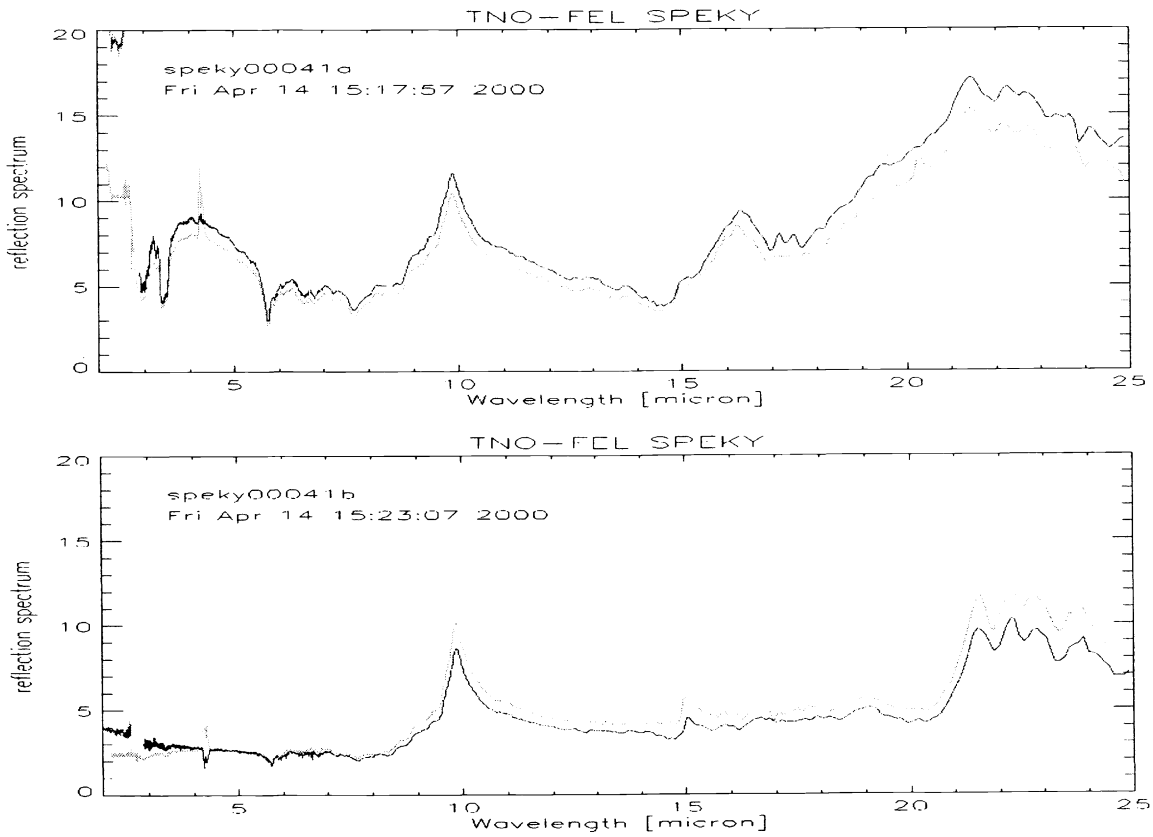

Figure 3: spectra of green (top) and black (bottom) painted plastic (reflection coefficient in % versus wavelength from 2 μm to 25 μm). The narrow emission/absorption at 4.3 μm is due to phase difference within the FTIR due to CO_2.

In Figure 3 spectra of two pieces of the same plastic but with different paints are presented. The top panel contains spectra from a piece of plastic with green paint applied on it. The button panel contains spectra from a piece of plastic with black paint applied on it. In each panel two spectra are presented. These spectra have been taken at different occasions. There is a clear difference between the spectra from the green and black painted plastic. Based on these spectra we find:

1. The spectra of the green paint exhibits several absorption features: 2.9, 3.5, 5.7, 8.7, 16.9, 17.3, 17.6, 22.0, 22.5, 23.3, 24.0, and 24.6 μm with a typical full-width-half-maximum of 0.1 μm;
2. The spectra of the black paint exhibits absorption features which are a subset of that for the green paint: 5.7, 22.0, 22.5, 23.3, and 24.6 μm with a typical full-width-half-maximum of 0.1 μm;
3. Both the green and black paint show a remarkably strong peak at 9.8 μm and a shallow absorption feature on right side with a minimum at 14.6 μm. The spectrum of the green paint rises again with a peak at 16.2 μm, whereas the spectrum of the black paint remains flat;

It is clear that the two paints have a significantly different spectrum and that a hyper spectral imager or a multi spectral sensor would be able to distinguish between the two. A dedicated multi spectral sensor designed to distinguish between the green and the black painted plastic should preferably operate in the 4 μm to 5 μm band, or measure the slope from 18 μm to 22 μm spectrum.

Field spectra

Field spectra are obtained of a car, a Honda Civic (regular sedan) with the engine running stationary and one by applying the choke (Figure 4), and a Boeing 737 taking off from Schiphol airport (Figure 5). From a first look at Figures 4 and 5 we note the prominence of CO_2 emission from 4.2 μm to 4.5 μm and CO from 4.45 μm to 4.95 μm. These two molecules are both present in the atmosphere and in the exhaust gasses of a car and an aircraft.

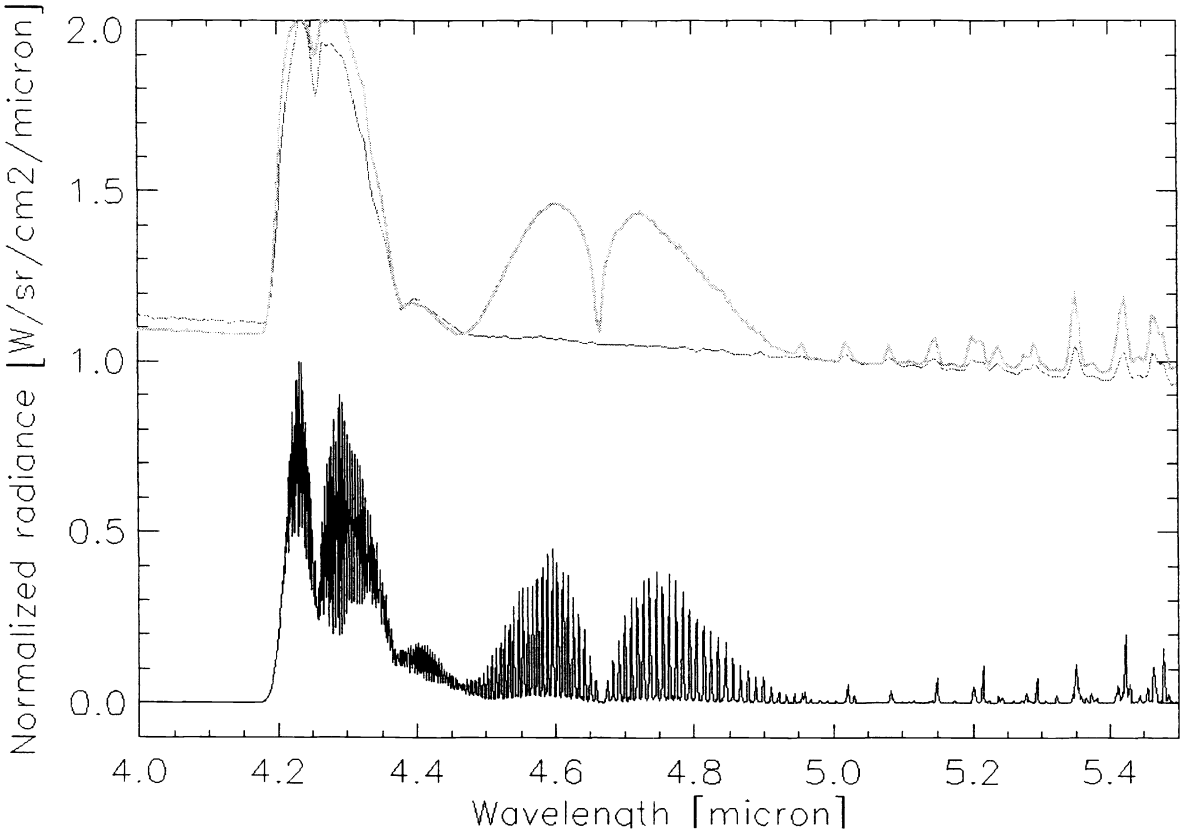

Figure 4: normalized emission spectra of car exhaust. The upper panel shows measured spectra for normal operating conditions (normal line) and with choke applied (thick line). The lower panel shows theoretical spectra of the molecules ($^{12}CO_2$, CO, and H_2O) extracted from the EPA database [5]. The $^{13}CO_2$ spectrum has been computed from the $^{12}CO_2$ spectrum by applying an isotopic shift of -60 cm^{-1}.

In Figure 4 emission spectra of the exhaust gas of a car, a regular Honda Civic (sedan) are presented. The CO_2 emission line is resolved in a R (4.25 μm) and P (4.30 μm) branch [6] with a weak emission line at 4.4 μm. Water vapor emission lines (H_2O) from 5.0 μm to 5.9 μm are clearly present. The two spectra correspond to engine setting: stationary and stationary with extra fuel added to the engine by applying the choke. The result of applying the choke is a significant increased emission of CO and enhanced emission of water. The R and P branch of CO are resolved at 4.60 μm and 4.75 μm respectively. The isotopic shift for $^{13}CO_2$ has been obtained from the HITRAN96 [7] molecular database (the wavenumber for minimum between the P and R branch intensity of the $^{12}CO_2$ and $^{13}CO_2$ fundamentals are respectively 2340 cm^{-1} and 2280 cm^{-1}) as -60 cm^{-1}. The isotope ratio of $^{12}CO_2/^{13}CO_2$ =89. The intensity ratio between emission from $^{12}CO_2$ and $^{13}CO_2$ does not fit ratio because the $^{12}CO_2$ is optically thick while $^{13}CO_2$ is optically thin. If no isotopic number is given, we assume it to be the main isotope. So CO_2 refers to $^{12}CO_2$.

In summary we find:

1. $^{12}CO_2$ fundamental emission at 4.25 μm (R branch) and 4.30 μm (P branch);
2. $^{13}CO_2$ weak emission line at 4.4 μm (P branch centered on 2274 cm^{-1})
3. ^{12}CO emission at 4.60 μm (R branch) and 4.75 μm (P branch);
4. H_2O emission from 5.0 μm to 5.9 μm.

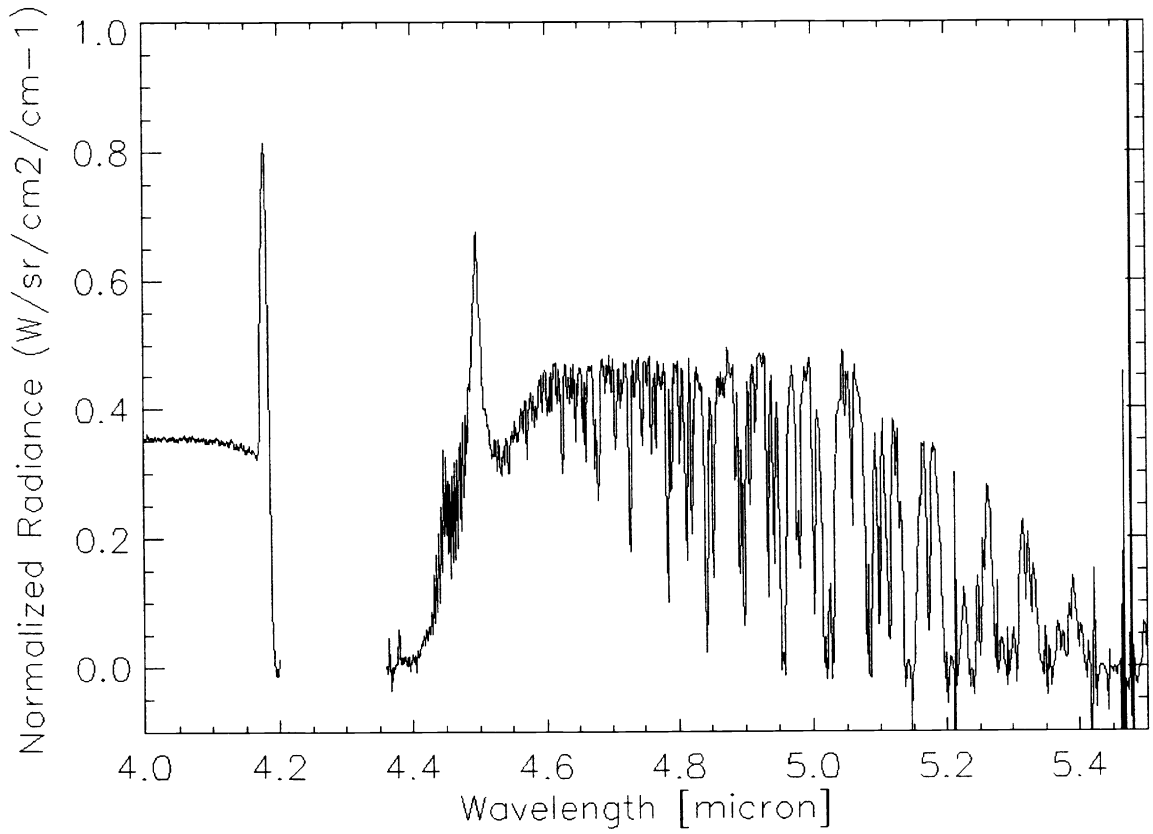

Figure 5: emission spectrum of a civilian Boeing 737 taking off from Schiphol airport. CO_2 atmospheric absorption in the 4.2 μm and 4.35 μm band is 100 % for a distance of more than a few meters. The measured spectrum does not contain information in that band and is therefore not displayed in the figure.

In Figure 5 a single emission spectrum from a time sequence (150 spectra in 30 seconds) of spectra (1700 cm^{-1} to 7000 cm^{-1} at 1 cm^{-1} spectral resolution) is presented of a track on a Boeing 737 taking off from Schiphol airport. The exhaust gas of the aircraft contains a large amount of CO_2 that will result in an emission line. The spectra was recorded when the the aircraft was at a distance of approximately 2 km and as a result CO_2 from the intervening atmosphere absorbs the aircraft's CO_2

emission. Since the temperature of the exhaust gas (T_{gas} = 500 K) is significantly hotter than that of the intervening atmosphere ($T_{atmosphere}$ = 288 K), the emission line will be significantly broader than the absorption line. The result is a blue (4.18 μm) and red (4.50 μm) CO_2 spike with a full-width-half-maximum of approximately 0.008 μm. The red and blue spikes of CO_2 are well known characteristics of hot exhaust gases. The distance between the two spikes is a measure for the temperature of the exhaust gas and possibly an indicator for the engine type. It would be of great interest to collect similar spectra for other aircraft types and engine types to find discriminating spectral characteristics (for a more detailed discussion we refer to [8]).

From Figure 5 we also note that there is significant continuum emission (no spectral features and resembling a blackbody spectrum) for wavelengths lower than 4.18 μm and for wavelengths larger than 4.6 μm. This continuum is attributed to emission of infrared radiation by hot engine parts within the field of view of the spectroradiometer. The narrow absorption lines for wavelength longer than 4.6 μm are due to water present within the intervening atmosphere. Furthermore we note that no CO emission (at 4.7 μm) was detected.

In order to develop a dedicated multi spectral sensor to detect missiles (or more accurate, their hot exhaust gas) it would be sufficient to measure the intensity of an emission line which is unique for a category of targets (those with a hot plume). For example, the intensity of the red or blue spike relative to the intensity in a spectral band without emission lines (in Figure 5, the 4.0 to 4.1 μm spectrum would be adequate although this contains thermal radiation from hot engine parts). If one would like to measure thermal infrared radiation (the continuum in Figure 5), a dedicated multi spectral sensor is not required and traditional infrared cameras can be used.

5. ATMOSPHERIC TRANSMISSION

Any hyper spectral data of a target at a range larger than several centimeters will be affected by atmospheric absorption, emission, and scattering and is dependent of the range to the target. Hence the effect is that atmospheric spectral data is of important for two reasons. Firstly for understanding and optimizing the target contrast for a target at a specific range. Secondly for improving passive range information of the detected target.

The six standard MODTRAN [9] environmental models have been used: tropical atmosphere, midlatitude summer, midlatitude winter, subarctic summer, subarctic winter, and 1976 US standard. Transmission spectra over a horizontal path length of 10 km at height of 10 meters (5 km visibility with rural aerosols) with a spectral resolution of 1 cm^{-1} are presented in Figure 6. For analysis purposes MODTRAN model in the mid-wave infrared (MWIR) 3 μm to 5 μm (3333 cm^{-1} to 2000 cm^{-1}) and the long-wave infrared (LWIR) 8 μm to 12 μm (1250 cm^{-1} to 833 cm^{-1}) bands has been computed. Obviously, these can only be crude estimates for extinction for targets, backgrounds and sensors that have high spectral resolution. Note that the LWIR band shows stronger dependence on the atmosphere type than the MWIR band. This is due to the increase in absolute water vapor content in the warmer scenarios. It becomes clear that the MWIR band is much more stable for an increase in water in the line of sight. Hence, in warm-humid conditions the MWIR band performs relatively well at longer ranges. This is confirmed in TNO-FEL experiments in the Caribbean area in 1999 [10].

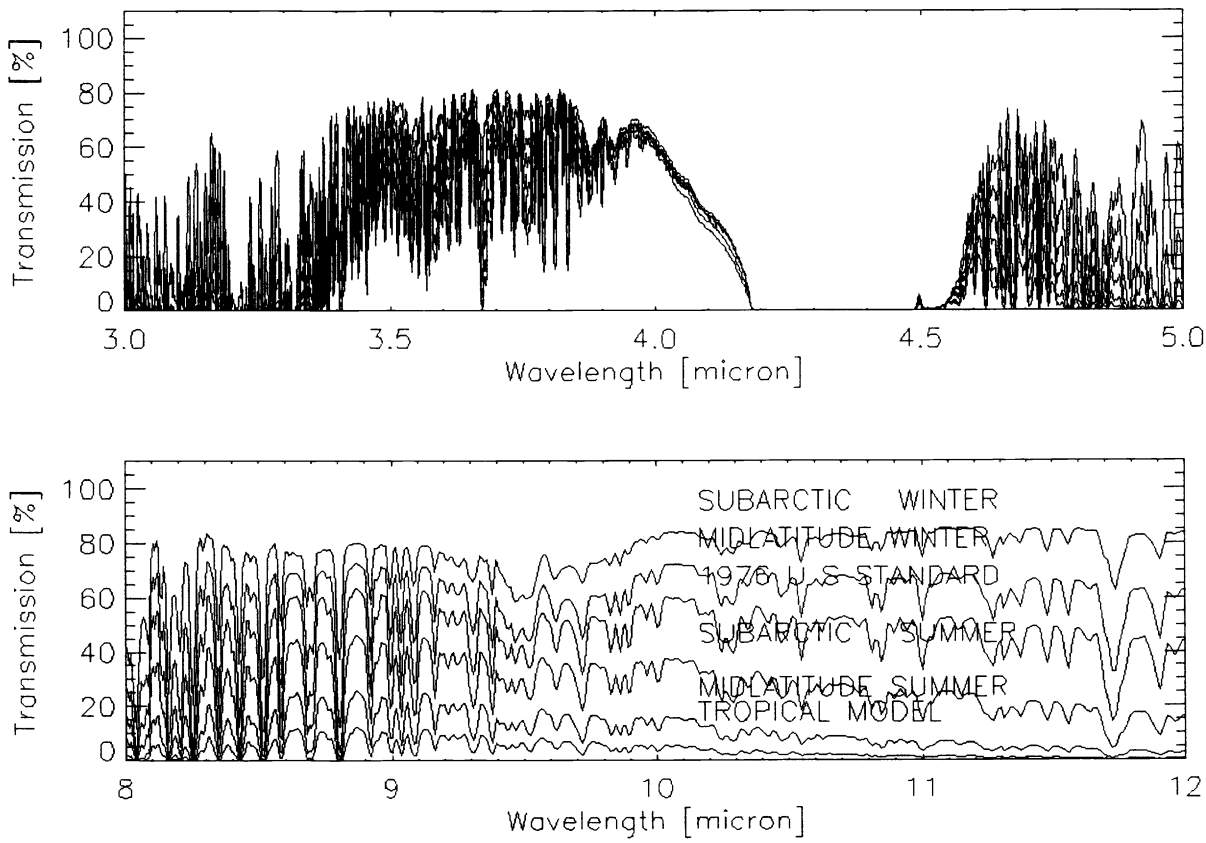

Figure 6: transmission values (%) over 10 km for the six standard MODTRAN atmospheres in the MWIR and LWIR bands. Transmission is presented versus wavelength (μm) in two atmospheric windows. Note the relatively strong dependence of the 8 μm to 12 μm band on the atmosphere type and the relatively independence in the 3.0 μm to 5.0 μm band.

6. PASSIVE RANGING

A novel approach to passive ranging is to make use of the spectral absorption due to the intervening atmosphere. This method takes advantage of the variations of atmospheric absorption with range. For target which emit a blackbody (a missile), the shape of the transmission can be relatively well determined. In the 3 μm to 5 μm window there are a number of characteristic narrow absorption bands caused by CO_2, CO, H_2O, and N_2O. Figure 7 shows transmission spectra calculated with MODTRAN for a selected section of the MWIR band (4.8 μm to 4.55 μm, 2450 cm^{-1} to 2200 cm^{-1}). Spectra at 2 cm^{-1} resolution are shown for 1 km, 2.5 km, 5 km, 10 km, and 20 km range. It is clear that the shape of the spectra contains information on the range. Note that although the absolute transmission value might be even more dependent on the range, this cannot be used for ranging because this assumes a priori knowledge on the target radiant intensity [11].

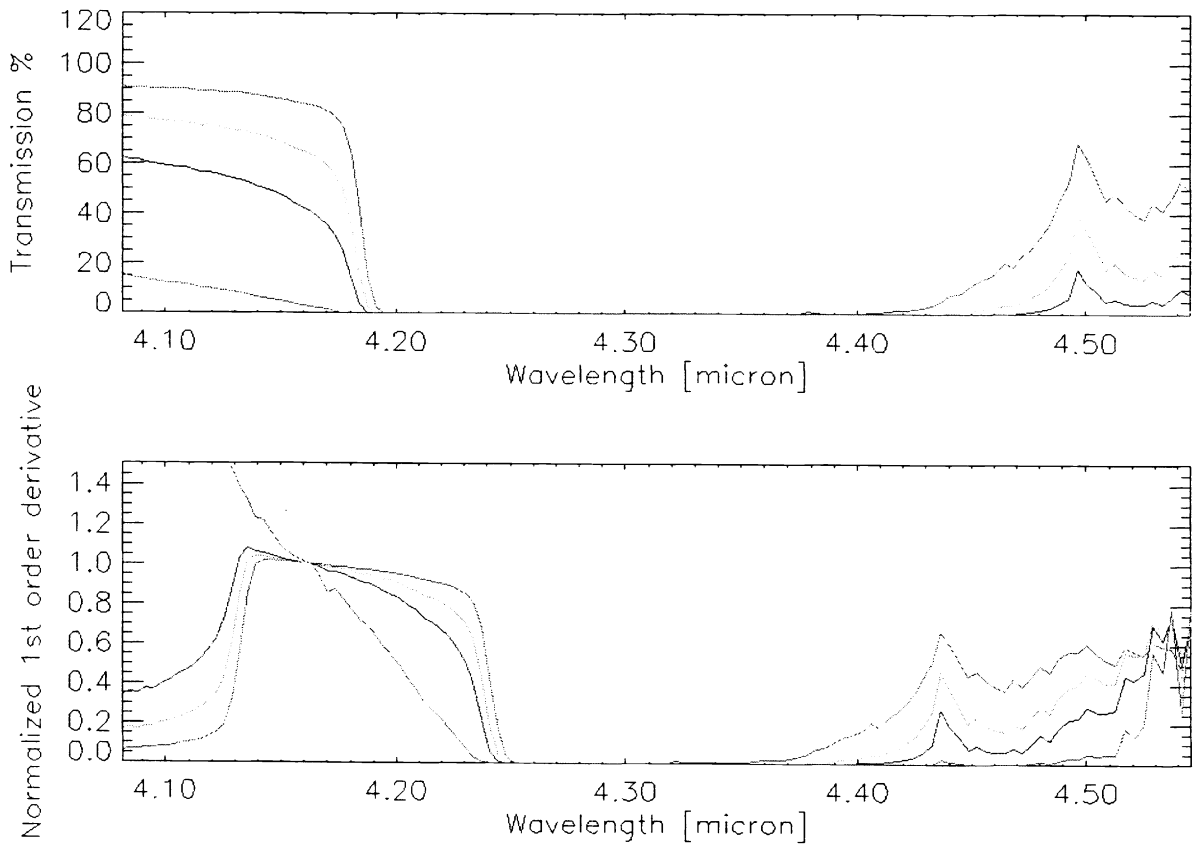

Figure 7: transmission spectra and normalized 1st order derivative of the transmission spectrum for a path length of 1 km, 2.5 km, 5 km, 20 km, and 20 km (at a height of 10 meter, subartic summer). The MODTRAN spectral resolution was 2 cm^{-1}, but spectra are smoothed to remove small-scale structures (spikes).

Spectra with better resolution (between 0.1 cm^{-1} and 1.0 cm^{-1}) can resolve even the individual molecular absorption lines. Intensity ratios between adjacent lines of one molecular band and intensity ratio's between different bands contain much more information on the range over which the transmission is measured. However, to obtain sufficient signal-to-noise ratio at these spectral resolutions in order to determine the range with some accuracy, dedicated Fourier Transform Infrared Spectrometers (FTIR) with large aperture are required. Even an FTIR instrument with an entrance pupil of 30 cm diameter would need 10 to 30 seconds to acquire one spectrum.

The use of more coarse spectra of for example 2 cm^{-1} resolution looks more promising. The position of the edge of the absorption band of CO_2 at the band head near 4.2 μm (2400 cm^{-1}) shows a range-dependence (Figure 7). Rather than fine tuning the method for passive ranging with spectral information an estimate of the required signal to noise ratio of the instrument will be given. To obtain intensity insensitive information the derivative of the spectra is taken and the derivative is normalized to the peak value in a given range. Results for a spectrum of a resolution of 2 cm^{-1} in the 4.08 μm to 4.55 μm (2450 to 2200 cm^{-1}) are shown in the lower panel of Figure 7 for 1 km, 2.5 km, 5 km, 10 km, and 20 km. From this information the range can be determined. It is estimated that one needs a signal-to-noise ratio of at least 100 to obtain a useful value for the range.

One has to bear in mind that in reality a spectrometer will not only measure the radiation of remote objects transmitted through the atmosphere, but also the path radiance between the object and the instrument. In the region between 4.2 μm and 4.3 μm (2325 cm^{-1} and 2380 cm^{-1}) the CO_2 in the atmosphere is optically thick and effectively the spectrometer "sees" blackbody radiation at the temperature of the ambient air. This indicates that the method can only be useful for ranging of

objects significantly warmer than the ambient air. Nose cones of high-speed missiles and exhaust gases might fulfil this condition.

To determine the feasibility a FTIR like instrument is considered. An information update rate of 1 sec, and a resolution of 2 cm^{-1} is assumed. For a conventional FTIR system this requires an optical path difference of 0.5 cm. To complete this displacement within 1 second, a variation of optical path length of 0.5 cm/sec is required. A spectral bandwidth from 6.7 μm to 2.5 μm (1500 cm^{-1} to 4000 cm^{-1}) will thus be converted into an electronic bandwidth for the detector of 750 to 2000 Hz. Assuming a background limited InSb detector of 1 mm^2 area with D* of 5 10^{11} $cmHz^{½}/W$. Converting these data into a detector noise equivalent power (NEP), taking into account the signal-to-noise ratio and the optics losses in the instrument (0.2), one needs 5 10^{-9} W at the entrance pupil of the instrument. Converting this to spectral power one needs 5 10^{-11} to 5 10^{-12} W/cm^{-1}.

For ranging of a target area A_{target} with radiance S at range R with an instrument entrance pupil A_{pupil} through an atmosphere τ_{atm} one obtains the following equation:

$$(A_{target}\, S / R^2)\, A_{pupil}\, \tau_{atm} > 10^{-11}\ W/cm^{-1}$$

For 10 km range, 0.02 m^2 pupil area, and a τ_{atm} of 0.5, the product A_{target} S must exceed 0.1. The table below gives some typical values. A 1 m^2 target at 500 K fulfils this condition. The intensity at 500 K is high enough to ignore the path radiance at 280 to 300 K.

Table 1: spectral radiance at 4.1 μm (2400 cm^{-1}) for a range of target temperatures.

Temperature (K)	Spectral Radiance ($W/m^2/sr/cm^{-1}$) at 2400 cm^{-1}
280	0.00073
300	0.0017
400	0.029
500	0.16
600	0.53
700	1.2

In conclusion passive ranging by use of spectral information seems feasible for a not too large instrument. The benefit of this application would be to have a completely passive and hence covert method of determining the target range.

7. DISCUSSION

Hyper spectral imaging is a powerful technique for research and development purposes. The TNO-FEL approach is to use a hyper spectral imager to determine spectral signatures of targets and backgrounds, and to develop detection and classification algorithms. These activities should then result in a design of a dedicated multi spectral sensor for detection and classification of targets.

Two applications of dedicated sensors are of interest regarding this paper. Those to increase the detection range of point source target at large distance (e.g. missiles), and those to classify and to identify targets (spatially resolved targets at close distance). While in the first case clutter and target strengths and signal to noise ratio are key factors, for the latter the unique spectral features of materials are of importance.

Due to environmental effects, aspect angles, the intervening atmosphere, scene reflection, and other effects, spectral data recorded with a hyper spectral imager is more complex than those recorded using laboratory spectrometers. In order to study spectral features of materials that are not affected by environmental effects, TNO-FEL is developing a database (referred to as SPEKY) of laboratory and field single point spectra in order to support hyper spectral imaging activities.

The laboratory reflection spectra presented in Figures 2 and 3 (and those in the SPEKY database) are superior in quality both in signal-to-noise ratio as in spectral resolution to data obtained with a hyper spectral imager. From an analysis of the spectra of those presented in this paper we find that there are many distinct features present. Identification of these features

is of importance for a discussion on false alarm rates. We also noted that the absolute value of the reflection coefficient is sensitive to the instrument performance. Some suggestions are made on the preferred band to detect or identify these targets.

The field emission spectra presented in Figures 4 and 5 show that emission lines from CO_2, $^{13}CO_2$, CO, and H_2O, and thermal emission from hot targets can be used for target detection. The presence of these lines is indicative for the presence of a target. However, to classify a target with these data is much more complicated. As an example we present data that could be used to identify emission of CO (a pollutant of the environment) by cars.

The presented analysis of the small set of spectra show that there are unique spectral features that can be used to improve detection range or classification of targets using a dedicated multi spectral sensor.

A study on the propagation of radiation through the intervening atmosphere is presented. The best window for what concerns transmission depends on absolute humidity, expected clutter, and required range. This cannot be answered in a trivial manner. The present idea is to optimize for detection and reduce the false alarms later, hence the mid-wave infrared would become preferable.

An example of passive ranging is given using the normalized 1st order derivative of the CO_2 atmospheric absorption line. This method could be applied to hyper spectral imaging data in order to correct the data for atmospheric effects. With this approach an accurate covert method becomes available of determining target ranges. This is clearly beneficial in scenarios when a platform would like to be able to control its emission in all cases.

When hyper spectral imagers will become readily available and robust algorithms are developed to detect, to classify, and even to identify targets, this will pose new challenges for camouflage and countermeasures techniques. It will become increasingly difficult to camouflage a target by applying a paint that resembles the background. Alternative methods such as obscuration might gain popularity.

8. ACKNOWLEDGEMENTS

The Royal Netherlands Army, Royal Netherlands Airforce, and Royal Netherlands Navy supported this work. The authors would like to thank Dr. H.M.A. Schleijpen for his kind assistance and advise to the authors regarding the passive ranging method.

9. REFERENCES

[1] Schau H.C.: 1981, Spectral discrimination, Infrared physics Vol. 21, pp 65-78
[2] Bakker E.J.: 1998, Hyperspectral imaging at TNO-FEL, TNO report, FEL-98-B303
[3] Schleijpen H.M.A., Craje M.W., Eisses S.M.: 1993, Proc. SPIE Vol. 2020, pp 225-233
[4] Dion D., Thériault J.-M., Hutt D., Forand L.: 1997, Canadian contribution to the Low-Altitude Point-Target Experiment (LAPTEX), DREV-TM-9706
[5] United States Environmental Protection Agency (http://www.epa.gov/ttnemc01/ftir)
[6] Bernath P.F.: 1995, Spectra of Atoms and Molecules, Oxford University Press, ISBN 0-19-507598-6
[7] Rothman L.S.: 1996, HITRAN
[8] Heland J., and Schäfer K.: 1997, Applied Optics Vol. 36, No 21.
[9] Kneizys F.X., Abreu L.W., Anderson G.P., Chetwynd J.H., Shettle E.P., Berk A., Bernstein L.S., Robertson D.C., Acharya P., Rothman L.S., Selby J.E.A., Gallery W.O., and Clough S.A.: 1996, The MODTRAN 2/3 Report and LOWTRAN 7 Model
[10] Schwering P.B.W, de Jong A.N., Winkel J., Kemp R.A.W.: 2000, The WATIX experiment, TNO-FEL report in preparation
[11] Schleijpen H.M.A., Neele F.P., de Grootte F.P.J., van Eijk A.M.J.: 1998, SHEPHARD NIGHT VISION conference